# Perturbed Quad-Rotor Trajectory Control Using Only Position and Yaw Sensors

## Mohammed Alfayizi[1], Yuri Shtessel[2]

*[1, 2] Electrical and Computer Engineering, The University of Alabama in Huntsville, AL, UAS*

**Abstract:** *This paper presents a novel trajectory control design for perturbed Quad-Rotor Unmanned Aerial Vehicle (QR-UAV) using generalized relative degree approach that reduces the need for all dix sensors of QR-UAV states to four sensors position $(x, y, z)$ and yaw angle ($\psi$). Super-Twisting (STW) control was applied for controlling the yaw angle ($\psi$) in the presence of smooth perturbations with bounded derivatives. Continuous High Order Sliding Mode (CHOSM) control was used for controlling the position states $(x, y, z)$, in a single loop in the presence of smooth perturbations with bounded derivatives. The proposed single loop SWT and CHOSM controllers drive the position trajectory and yaw tracking errors to zero asymptotically. The finite convergent time HOSM differentiators were used to facilitate the CHOSM controllers. The proposed single loop sliding mode controllers were validated via simulations.*

**Keywords:** *Quad-Rotor control, Sliding Mode Control, Continuous HOSM, Perturbations.*

## 1. Introduction

In the last decade, the Quad-Rotor (QR) became the most popular unmanned aerial vehicle (UAV) version because of its advantages such as low cost, small size, stable hovering, and simple construction and maintenance. These advantages make QR suitable for many civil applications such as agriculture, filming, or military missions, among others. These different missions require a controller that offers stability and robustness for the QR to work properly in different environments, including bounded perturbations, which is the most challenge task in the QR controller design. This challenge was addressed in the literature with a verity of solutions for different aims. In the literature, a large variety of QR controllers were discussed. They include linear controllers, for instance, PI and PID ones, which are not capable of mitigating casual perturbations [1]. Other types of controllers include feedback linearization [2], linear quadratic regulator (LQR)[3], and a variety of nonlinear control laws that take care of disturbances such as robust adaptive tracking control[4], neural network[5], or sliding mode control (SMC) [6].

QR-UAV is an under-actuated system where the number of control inputs is fewer the number of controlled outputs. Because of this, designing the

decoupling controller is complicated. Usually a cascade controller with multiple loops is used to handle this under-actuated control problem. The outer loop controller controls the QR position, and the inner loop controller is used to stabilize the attitude. For a multiple loop control structure, all six sensors are used. The large number of sensors increases the probability of the sensor failure, which yields the loss of QR. Furthermore, these multiple-loop structure require time-scale separation where the inner loops should be faster than the outer loops[7][8].

On the other hand, using only four sensors and applying the relative degree approach with dynamic extension[9][10] to control the QR-UAV allows designing a control structure that uses only a single loop controller. In the work [11], there is an attempt to use only four sensors. The work of [11] designed a controller that used only the altitude ($z$) and attitude angles ($\phi, \theta, \psi$) sensors and use an observer that uses Euler angles ($\phi, \theta, \psi$) and their derivatives to estimate $x$ and $y$ which is believed that the controller does not compensate for external disturbances on $x$ and $y$ because they are estimated by other states.

The single-loop controller that is studied in this work has some expected advantages with respect to the multiple-loop controller. The main advantage is in reducing the number of measurements and sensors used in the feedback loop. Another important advantage is in square configuration that is equivalent to a fully actuated system. Last but not the least, an expected advantage is the avoidance of time-scale separation between control loops [7][8].

To the best of authors' knowledge, there is no work in the literature where a single loop controller operates in the presence of perturbations.

The contribution of this work is in

1) Proposing a single-loop robust output tracking control approach using only four sensors for QR-UAV using generalized relative degree approach.

2) Designing the single-loop controller for a 6 DOF QR-UAV perturbed mathematical model in terms of STW and CHOSM controls that drive output tracking errors asymptotically to zero in the presence of the bounded perturbations.

3) Validating the designed STW and CHOSM controllers via simulations of 6 DOF perturbed dynamic model of QR-UAV.

The reminder of this paper is structure as follows. In Section 2, the mathematical model of the QR-UAV is shown. The problem is formulated in Section 3. The single-loop controller design, is presented in Section 4. The simulation results and conclusion are presented in Section 5 and Section 6, respectively.

## 2. Quad-Rotor Dynamics

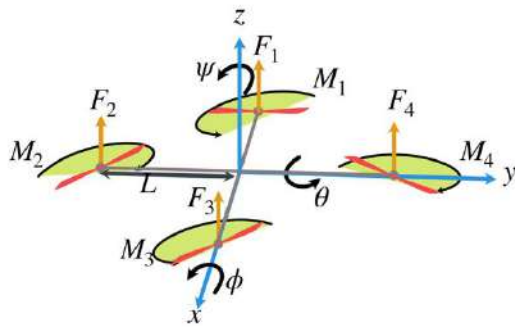The QR-UAV dynamics are described by the system of differential equations[12]



**Fig -1**: Schematic view and variable definitions of QR.

$$\ddot{x} = \left(C_\phi S_\theta C_\psi + S_\phi S_\psi\right)\frac{U_1}{m} + d_x$$
$$\ddot{y} = \left(C_\phi S_\theta S_\psi - S_\phi C_\psi\right)\frac{U_1}{m} + d_y \qquad (1)$$
$$\ddot{z} = \left(C_\phi C_\theta\right)\frac{U_1}{m} + d_z$$

$$\ddot{\phi} = \left(\frac{I_{yy} - I_{zz}}{I_{xx}}\right)\dot{\theta}\dot{\psi} - \frac{J_r}{I_{xx}}\dot{\theta}\Omega + \frac{U_2}{I_{xx}} + d_\phi$$
$$\ddot{\theta} = \left(\frac{I_{zz} - I_{xx}}{I_{yy}}\right)\dot{\phi}\dot{\psi} + \frac{J_r}{I_{yy}}\dot{\phi}\Omega + \frac{U_3}{I_{yy}} + d_\theta \qquad (2)$$
$$\ddot{\psi} = \left(\frac{I_{xx} - I_{yy}}{I_{zz}}\right)\dot{\theta}\dot{\phi} + \frac{U_4}{I_{zz}} + d_\psi$$

Where $C_{(:)} = cos(:)$ and $S_{(:)} = sin(:)$. The state $x, y$ and $z$ represent the $x-$axis, $y-$axis, and $z-$axis respectively (m), and $\phi, \theta$ and $\psi$ represent roll, pitch, and yaw respectively in Euler angles (rad). The differentiable external bounded disturbances are $d_x, d_y, d_\phi, d_\theta$ and $d_\psi$. The other parameters are defined as follows: $m$ is mass of QR (kg); $g$ is gravitational acceleration; $I_{xx}, I_{yy}$, and $I_{zz}$ are moment of inertia around $x-$ axis, $y-$ axis, and $z-$axis respectively $(kg.m^2)$; and $J_r$ is the propeller inertia coefficient.

The control force acting on $z-$axis is $U_1$ and $U_2, U_3$, and $U_4$ are the control torques around $x-$axis, $y-$axis, and $z-$axis respectively.

The controls are computed as follows:

$$U_1 = \sum_{i=1}^{4} F_i$$
$$U_2 = L(F_2 - F_4)$$
$$U_3 = L(F_1 - F_3) \qquad (3)$$
$$U_4 = -M_1 + M_2 - M_3 + M_4$$
$$\Omega = -\Omega_1 + \Omega_2 - \Omega_3 + \Omega_4$$

Where the force $F_i = b\Omega_i, i = 1,2,3,4; b$ is thrust coefficient; $\Omega_i$ is the angular velocity of propeller $i$ in Fig. 1; $L$ is the distance between the motor and center of gravity $(m)$; the torque $M_i = d\Omega_i$; and $d$ is drag coefficient. All forces and torques are generated by propellers 1,2,3, and 4 shown in Fig. 1. The dynamics of the propeller actuators are not considered.

## 3. Problem Formulation

The problem to be consider is: Given the mathematical model of QR-UAV in Eqs. (1)-(3) design a single-loop feedback control in terms of $U_1, U_2, U_3$, and $U_4$ so that

$$x \to x_c, y \to y_c, z \to z_c, \psi \to 0 \qquad (4)$$

As time increases in the presence of the bounded perturbations, where $x_c(t), y_c(t)$, and $z_c(t)$ are commanded position trajectory profiles, smoothly generated on-line, to be followed by $x, y$, and $z$.

**Remark 1:** *The problem in (4) is a fully actuated control problem, since the number of controlled outputs is equal to the number of control inputs.*

## 3. The Single-Loop Controller Design

### 3.1 The QR yaw angle ψ input-output dynamic

The dynamic equation of $\psi$ is already presented in input-output dynamical format in system (1)-(2) with relative degree $r_\psi = 2$. No dynamic extension[9][10] is needed here. It is rewritten as

$$\ddot{\psi} = \alpha_\psi U_4 + \left(\frac{I_{xx} - I_{yy}}{I_{zz}}\right)\dot{\theta}\dot{\phi} + d_\psi \qquad (5)$$

Where $\alpha_\psi = \frac{1}{I_{zz}}$.

Assume that QR dynamics in (5) can be uncertain. Therefore, the following assumption is made:

**Assumption 1:**

$$\alpha_\psi = \alpha_{\psi_0} + \Delta\alpha_\psi$$

*Where* $\alpha_{\psi_0}$ *represents a known nominal value of* $\alpha_\psi$, *while* $\Delta\alpha_\psi$ *is uncertain terms so that* $\left|\frac{\Delta\alpha_\psi}{\alpha_{\psi_0}}\right| < 1$.

Supposing **Assumption 1** holds, Eq (5) is rewritten as

$$\ddot{\psi} = u_\psi + \zeta_\psi \qquad (6)$$

Where

$$u_\psi = \alpha_{\psi_0} U_4$$

$$\zeta_\psi = \left(\frac{I_{xx} - I_{yy}}{I_{zz}}\right)\dot{\theta}\dot{\phi} + \Delta\alpha_\psi U_4$$

The control function $u_\psi$ is to be designed to drive $\psi \to 0$, as time increases in the presence of perturbations and the bounded derivative $\dot{\zeta}_\psi$. Note that it is a single-loop control configuration that is commonly used [1]-[6]. The controller $u_\psi$ is described in detail in Section 3.3.

### 3.2 The QR position $x, y,$ and $z$ input-output dynamics

In deriving these dynamics, the following assumption is made:

**Assumption 2:** *The angle* $\psi$ *described by (6) is assumed to be driven to zero by means of the control* $u_\psi$ *whose design is considered in next section.*

Therefore $x, y$, and $z$ input-output dynamics are derived using the generalized relative degree approach with dynamic extension[9][10] that is needed in order to obtain a non-singular control distribution matrix: specifically

$$x^{(4)} = (a_{11} + a_{12}U_2 + a_{13}U_3)U_1 + a_{14}\dot{U}_1$$
$$+ a_{15}\ddot{U}_1 + a_{16}d_\phi + a_{17}d_\theta$$
$$+ \ddot{d}_x$$
$$x^{(4)} = (a_{21} + a_{22}U_2)U_1 + a_{24}\dot{U}_1 + a_{25}\ddot{U}_1 \qquad (7)$$
$$+ a_{26}d_\phi + a_{27}d_\theta + \ddot{d}_y$$
$$x^{(4)} = (a_{31} + a_{32}U_2 + a_{33}U_3)U_1 + a_{34}\dot{U}_1$$
$$+ a_{35}\ddot{U}_1 + \ddot{d}_y$$

Where

$$a_{11} = \frac{J_r}{mI_{yy}}\dot{\phi}\Omega C_\theta C_\phi + \frac{J_r}{mI_{xx}}\dot{\theta}\Omega S_\theta S_\phi - \frac{1}{m}$$
$$(\dot{\theta}^2 + \dot{\phi}^2)S_\theta C_\phi - \frac{2}{m}\dot{\theta}\dot{\phi}C_\theta S_\phi$$

$$a_{12} = \frac{1}{mI_{xx}}S_\theta S_\phi; a_{12} = \frac{1}{mI_{yy}}C_\theta C_\phi$$

$$a_{14} = \frac{2}{m}(\dot{\theta}C_\theta C_\phi - \dot{\phi}S_\theta S_\phi); a_{15} = \frac{1}{m}S_\theta C_\phi$$

$$a_{21} = \frac{1}{m}\dot{\phi}^2 S_\phi + \frac{J_r}{mI_{xx}}\dot{\theta}\Omega C_\phi; a_{22} = -\frac{1}{mI_{xx}}C_\phi$$

$$a_{24} = -\frac{2}{m}\dot{\phi}C_\phi; a_{25} = -\frac{1}{m}S_\phi$$

$$a_{31} = \frac{2}{m}(\dot{\theta}\dot{\phi}S_\theta S_\phi - \frac{1}{m}(\dot{\theta}^2 + \dot{\phi}^2)C_\theta C_\phi + \frac{J_r}{mI_{xx}}\dot{\theta}\Omega C_\theta S_\phi$$
$$- \frac{J_r}{mI_{yy}}\dot{\phi}\Omega S_\theta C_\phi$$

$$a_{32} = -\frac{1}{mI_{xx}}C_\theta S_\phi; a_{33} = -\frac{1}{mI_{yy}}S_\theta C_\phi$$

$$a_{34} = \frac{2}{m}(\dot{\theta}S_\theta C_\phi - \dot{\phi}C_\theta S_\phi); a_{35} = \frac{1}{m}C_\theta C_\phi$$

The following assumptions are made about the perturbations terms in Eq. (7) for $a_{13}, a_{22}$, and $a_{35}$:

**Assumption 3:**

$$a_{kn} = a_{kn_0} + \Delta a_{kn} \qquad k, n = 1,2,3,4,5$$

*Where* $U_1 > 1$, *and* $a_{kn_0}$ *represents a known nominal value of* $a_{kn}$, *while* $\Delta a_{kn}$ *is uncertain terms so that* $\left|\frac{\Delta a_{kn}}{a_{kn_0}}\right| < 1$.

Eq. (7) is rewritten as

$$\begin{bmatrix} x^{(4)} \\ y^{(4)} \\ z^{(4)} \end{bmatrix} = \begin{bmatrix} 1 & 0 & 0 \\ 0 & 1 & 0 \\ 0 & 0 & 1 \end{bmatrix}\begin{bmatrix} u_x \\ u_y \\ u_z \end{bmatrix} + \begin{bmatrix} \zeta_x \\ \zeta_y \\ \zeta_z \end{bmatrix} \qquad (8)$$

Where

$$u_x = (a_{11_0} + a_{12_0}U_2 + a_{13_0}U_3)U_1 + a_{14_0}\dot{U}_1 + a_{15_0}\ddot{U}_1$$
$$\zeta_x = (\Delta a_{11} + \Delta a_{12}U_2 + \Delta a_{13}U_3)U_1 + \Delta a_{14}\dot{U}_1$$
$$+ \Delta a_{15}\ddot{U}_1 + a_{16}d_\phi + a_{17}d_\theta + \ddot{d}_x$$
$$u_y = (a_{21_0} + a_{22_0}U_2)U_1 + a_{24_0}\dot{U}_1 + a_{25_0}\ddot{U}_1$$
$$\zeta_y = (\Delta a_{21} + \Delta a_{22}U_2)U_1 + \Delta a_{14}\dot{U}_1 + \Delta a_{25}\ddot{U}_1$$
$$+ a_{26}d_\phi + a_{27}d_\theta + \ddot{d}_y$$
$$u_z = (a_{31_0} + a_{32_0}U_2 + a_{33_0}U_3)U_1 + a_{34_0}\dot{U}_1 + a_{35_0}\ddot{U}_1$$
$$\zeta_z = (\Delta a_{31} + \Delta a_{32}U_2 + \Delta a_{33}U_3)U_1 + \Delta a_{34}\dot{U}_1$$
$$+ \Delta a_{35}\ddot{U}_1 + a_{36}d_\phi + a_{37}d_\theta + \ddot{d}_z$$

Note that the control distribution matrix in Eq. (8) is equal to $I_{3\times3}$ and is therefore non-singular. As soon as the generalized control functions $u_x, u_y$, and $u_z$ designed, the original controls are to be identified based on Eq. (8).

The control input $U_1$ can be found from the filter in Eq. (9) and satisfied

$$\gamma_{z3_0}\ddot{U}_1 + \gamma_{z2_0}\dot{U}_1 + \gamma_{z1_0} = \gamma_{z4_0}u_x - \gamma_{z5_0}u_y + u_z \qquad (9)$$

Then, $U_2$ and $U_3$ are found from Eq. (10)

$$U_2 = \gamma_{x_0} + \gamma_{x1_0}\dot{U}_1 + \gamma_{x2_0}\ddot{U}_1 + \gamma_{x4_0}u_y$$
$$U_3 = \gamma_{y_0} + \gamma_{y1_0}\dot{U}_1 + \gamma_{y2_0}\ddot{U}_1 + \gamma_{y3_0}u_x \qquad (10)$$
$$+ \gamma_{y4_0}u_y$$

Where

$$\gamma_{x_0} = -\frac{a_{21_0}}{a_{22_0}}; \gamma_{x1_0} = -\frac{a_{24_0}}{a_{22_0}U_1}$$

$$\gamma_{x2_0} = -\frac{a_{25_0}}{a_{22_0}U_1}; \gamma_{x4_0} = \frac{1}{a_{22_0}U_1}$$

$$\gamma_{y_0} = \frac{a_{12_0}a_{21_0}}{a_{13_0}a_{22_0}} - \frac{a_{11_0}}{a_{13_0}}; \gamma_{y1_0} = \frac{a_{12_0}a_{24_0}}{a_{13_0}a_{22_0}U_1} - \frac{a_{14_0}}{a_{13_0}U_1}$$

$$\gamma_{y2_0} = \frac{a_{12_0}a_{25_0}}{a_{13_0}a_{22_0}U_1} - \frac{a_{15_0}}{a_{13_0}U_1}; \; \gamma_{x3_0} = \frac{1}{a_{13_0}U_1}$$

$$\gamma_{y2_0} = -\frac{a_{12_0}}{a_{13_0}a_{22_0}U_1}$$

$$\gamma_{z1_0} = \frac{a_{12_0}a_{21_0}a_{33_0}}{a_{13_0}a_{22_0}} - \frac{a_{11_0}a_{33_0}}{a_{13_0}} - \frac{a_{21_0}a_{32_0}}{a_{22_0}} + a_{31_0}$$

$$\gamma_{z2_0} = \frac{a_{12_0}a_{24_0}a_{33_0}}{a_{13_0}a_{22_0}} - \frac{a_{14_0}a_{33_0}}{a_{13_0}} - \frac{a_{33_0}a_{32_0}}{a_{22_0}} + a_{34_0}$$

$$\gamma_{z3_0} = \frac{a_{12_0}a_{25_0}a_{33_0}}{a_{13_0}a_{22_0}} - \frac{a_{15_0}a_{33_0}}{a_{13_0}} - \frac{a_{25_0}a_{32_0}}{a_{22_0}} + a_{35_0}$$

$$\gamma_{z4_0} = \frac{a_{33_0}}{a_{13_0}}; \; \gamma_{z5_0} = \frac{a_{33_0}}{a_{22_0}} - \frac{a_{12_0}a_{33_0}}{a_{13_0}a_{22_0}}$$

Note that based on the QR design and attitude angle physical constrains $\phi, \theta \in \left(-\frac{\pi}{2}, \frac{\pi}{2}\right)$, the values of $a_{13_0}$ and $a_{22_0}$ are never equal to zero, as well as $U_1 > 0$.

**Discussion:** *Due to dynamic extension in (8) the reconstruction of the control functions $U_1, U_2,$ and $U_3$ based on the controls $u_x, u_y$ and $u_z$ has a dynamic component as in Eqs. (9) and (10) . For stability of this dynamic transformation the coefficients $\gamma_{z3_0}, \gamma_{z2_0}$ and $\gamma_{z1_0}$ must be positive.*

**Remark 2:** *Knowledge of the QR attitude angles $\phi$ and $\theta$ are not required for the controller design.*

**Remark 3:** *The control laws in terms of $F_i$ and $M_i$ in accordance with Eq. (3) can be computed as soon as the control laws are designed in terms of $U_1, U_2, U_3$ and $U_4$.*

$$
\begin{bmatrix} F_1 \\ F_2 \\ F_3 \\ F_4 \end{bmatrix} =
\begin{bmatrix}
\frac{1}{4} & 0 & \frac{1}{2L} & -\frac{b}{4d} \\
\frac{1}{4} & \frac{1}{2L} & 0 & \frac{b}{4d} \\
\frac{1}{4} & 0 & -\frac{1}{2L} & -\frac{b}{4d} \\
\frac{1}{4} & -\frac{1}{2L} & 0 & \frac{b}{4d}
\end{bmatrix}
\begin{bmatrix} U_1 \\ U_2 \\ U_3 \\ U_4 \end{bmatrix}
$$

$$
\begin{bmatrix} M_1 \\ M_2 \\ M_3 \\ M_4 \end{bmatrix} =
\begin{bmatrix}
\frac{d}{4b} & 0 & \frac{d}{2bL} & -\frac{1}{4} \\
\frac{d}{4b} & \frac{d}{2bL} & 0 & \frac{1}{4} \\
\frac{d}{4b} & 0 & -\frac{d}{2bL} & -\frac{1}{4} \\
\frac{d}{4b} & -\frac{d}{2bL} & 0 & \frac{1}{4}
\end{bmatrix}
\begin{bmatrix} U_1 \\ U_2 \\ U_3 \\ U_4 \end{bmatrix}
\tag{11}
$$

Next, the control functions $u_x, u_y,$ and $u_z$ are to be designed to drive $x \to x_c, y \to y_c$ and $z \to z_c$ respectively, as time increases in the presence of the perturbations and the bounded derivatives $\dot{\zeta}_x, \dot{\zeta}_y$ and $\dot{\zeta}_z$. Note that this design yields a novel single-loop control configuration using only four sensors.

### 3.3 Designing the single-loop STW and CHOSM control

The tracking position and yaw angle errors are introduced as

$$e_x = x_c - x, e_y = y_c - y, e_z = z_c - z \text{ and } e_\psi = \psi_c - \psi.$$

The goal is to design the control functions $u_x, u_y, u_z,$ and $u_\psi$ to drive $e_j, j = x, y, z, \psi$ to zero in the presence of the bounded perturbations.

This work proposes the use of STW[13] and CHOSM control techniques[14] for designing the mentioned single-loop controllers. The designed controllers

- Drive the sliding variables of highest relative degree and their consecutive derivatives up to $r - 1$ to zero in finite time in the presence of the bounded perturbations where $r$ is the relative degree.

- Are continuous without an artificial increase of the relative degree.

#### 3.3.1 Sliding variable design

This work proposes the use of sliding variable in the form:

$$\sigma_j = \dot{e}_j + c_j e_j, \quad c_j > 0 \tag{12}$$

In accordance with Eqs. (6)-(8) and (12) the relative degree of $\sigma_\psi$ w.r.t $u_\psi$ is equal to one, and the relative degree of $\sigma_x, \sigma_y,$ and $\sigma_z$ w.r.t $u_x, u_y,$ and $u_z$ respectively are equal to 3.

#### 3.3.2 Single-loop STW control for $\psi$ channel:

The sliding variable dynamics in $\psi$ channel is given by

$$\dot{\sigma}_\psi = -u_\psi + \xi_\psi \tag{13}$$

Where

$$\xi_\psi = \ddot{\psi}_c - \zeta_\psi + c_\psi e_\psi$$

The following assumption is made

**Assumption 4:** *The $\dot{\xi}_\psi$ is bounded in reasonable QR flight domain, that is $\left|\dot{\xi}_\psi\right| \leq C_\psi$.*

The STW control used in $\psi$ channel [13][14] is

$$u_\psi = \lambda_\psi \left|\sigma_\psi\right|^{0.5} sign(\sigma_\psi) + v_\psi$$
$$\dot{v}_\psi = \Gamma_\psi sign(\sigma_\psi) \tag{14}$$

Where $\lambda_\psi = 1.5\sqrt{C_\psi}, \Gamma_\psi = 1.1C_\psi, \left|\dot{\xi}_\psi\right| \leq C_\psi$. Note that the STW control (13) drives the sliding variable to zero in finite time.

### 3.3.2 Single-loop CHOSM control for $x, y$, and $z$ channels:

Consider the sliding variable dynamics

$$\sigma_j^{(r_j)} = -u_j + \xi_j, j = x, y, z \tag{15}$$

Where $r_j = 3$ is relative degree of the sliding variable $\sigma_j$ w.r.t the controller $u_j$ and

$$\xi_j = j_c^{(4)} - \zeta_j + c_j e_j^{(3)}$$

The following assumption is made

**Assumption 5:** *The $\dot{\xi}_j$ is bounded in reasonable QR flight domain, that is $\left|\ddot{\xi}_j\right| \le C_j$.*

The CHOSM control function that drives $\sigma_j, \dot{\sigma}_j, \dots, \sigma_j^{(r_j-1)}$ to zero in finite time is designed in a form [14]

$$u_j = u_{b_j} + u_{s_j} \tag{16}$$

Where

$$u_{b_j} = \gamma_{j1}\left|\sigma_j\right|^{\eta_{j1}} sign(\sigma_j) + \gamma_{j2}\left|\dot{\sigma}_j\right|^{\eta_{j2}} sign(\dot{\sigma}_j) + \gamma_{j3}\left|\ddot{\sigma}_j\right|^{\eta_{j3}} sign(\ddot{\sigma}_j) \tag{17}$$

And

$$u_\psi = \lambda_j \left|s_j\right|^{0.5} sign(s_j) + v_j$$
$$\dot{v}_j = \Gamma_j sign(s_j) \tag{18}$$

Where the auxiliary sliding variable

$$s_j(t) = \ddot{\sigma}_j + \int u_{b_j}(\tau)d \tag{19}$$

The scalars $\gamma_{j1}, \gamma_{j2}$ and $\gamma_{j3}$ must be chosen such that the polynomial

$$p^3 + \gamma_{j3}p^2 + \gamma_{j2}p + \gamma_{j1}$$

Is Hurwitz and the scalars $\eta_{j1}, \eta_{j2}$ and $\eta_{j3}$ are chosen recursively as

$$\eta_{j_{i-1}} = \frac{\eta_{ji}\,\eta_{j_{i+1}}}{2\eta_{j_{i+1}} - \eta_{ji}} \quad i = 2,3$$

With $\eta_{j4} = 1$ and $\eta_{j3} \in (1 - \epsilon, 1)$. The value of $\epsilon \in (0,1)$ ensures the finite convergence, this value can be identified by tuning during the simulation and then verified experimentally.

**Remark 4:** *To facilitate the CHOSM controllers in (12), (16) and (19) the HOSM differentiators[13]are employed.*

## 4. Simulation and Results

The nominal values that the controllers operate with were determined at the hovering condition in a steady state where all attitude angles $\phi, \theta$, and $\psi$ and their velocities $\dot{\phi}, \dot{\theta}$ and $\dot{\psi}$ in nominal value condition are zero. So the original inputs are computed as

$$U_1 = \frac{1}{\gamma_{z3_0}} \int\int u_z(\tau)d\tau_1 d\tau_2 + mg$$
$$U_2 = \gamma_{x4_0} u_y$$
$$U_3 = \gamma_{y4_0} u_x$$
$$U_4 = \frac{1}{\alpha_{\psi_0}} u_\psi \tag{20}$$

Where $mg$ is the initial force.

### 4.1 Simulation Setup

The system in Eqs. (1)-(3) parameters are presented in Table 1.

Table 1: The Parameters of The QR-UAV

| L | 0.3 m |
|---|---|
| m | 0.8 kg |
| g | $9.81\ m/s^2$ |
| $I_{xx}$ | $15.67 \times 10^{-3}$ |
| $I_{yy}$ | $15.67 \times 10^{-3}$ |
| $I_{zz}$ | $28.346 \times 10^{-3}$ |
| b | $192.32 \times 10^{-7} Ns^2$ |
| d | $4.003 \times 10^{-7} Nms^2$ |
| $J_r$ | $6.01 \times 10^{-5}$ |

To study the study the performance of the controllers designed in this work, Matlab and Simulink were used for simulation. The Euler integration algorithm was used with a step size equal to $10^{-4}s$. For simulation purpose, the bounded disturbances that were applied to the system (1)-(2) are

$$d_x = cos(t) + sin(2t)$$
$$d_y = sin(t) + cos(2t)$$
$$d_z = cos(0.5t)$$
$$d_\phi = 0.5cos(t)$$
$$d_\theta = 0.7cos(t)$$
$$d_\psi = 0.3cos(t)$$

The initial values are

$$[x_0, y_0, z_0, \phi_0, \theta_0, \psi_0] = \left[2, -1, 2, -\frac{\pi}{8}, \frac{\pi}{8}, \frac{\pi}{8}\right]$$

To meet the Hurwits condition for the polynomial in (17), ITAE Criterion[15]was applied with

$\omega_{n_x} = \omega_{n_y} = 1$ and $\omega_{n_z} = 2$. The parameter of the STW and CHOSM controllers in Eqs. (14) and (17)-(19) are given in Table 2.

Table 2: The Parameters of The Controllers

| $c_z$ | 1 | $\gamma_{j1}$ | $\omega_{n_j}^3$ |
|---|---|---|---|
| $c_\psi$ | 2 | $\gamma_{j2}$ | $2.15\,\omega_{n_j}^2$ |
| $c_x$ | 2 | $\gamma_{j3}$ | $1.75\omega_{n_j}$ |
| $c_y$ | 2 | $\eta_{j1}$ | 0.56 |
| $C_z$ | 10 | $\eta_{j2}$ | 0.66 |
| $C_\psi$ | 10 | $\eta_{j3}$ | 0.8 |
| $C_x$ | 10 | $C_y$ | 10 |

The desired trajectory is

$$[x_c, y_c, z_c] = [8cos(0.2t), 8sin(0.2t), sin(t) + 6]$$

### 4.2 Simulation Results

The QR position trajectories tracking in the presence of the bounded perturbations is demonstrated in **Fig -2**. The position tracking errors are demonstrated in **Fig -3**. The high accuracy tracking is achieved. The STW and CHOSM control profiles are presented in **Fig -4**. The controls have reasonable magnitudes that can by easy executed by the actuators. The corresponding attitude angle profiles are shown in **Fig -5**. The attitude angle profiles fall into the imposed limits: $\phi, \theta \in \left(-\frac{\pi}{2}, \frac{\pi}{2}\right)$. The sliding variable evolutions are shown in **Fig -6**. The sliding variables have reached zero in finite time by means of STW and continuous HOSM controllers in the presence of the bounded disturbances.
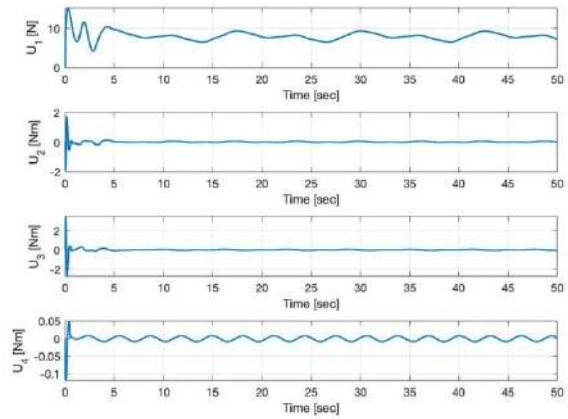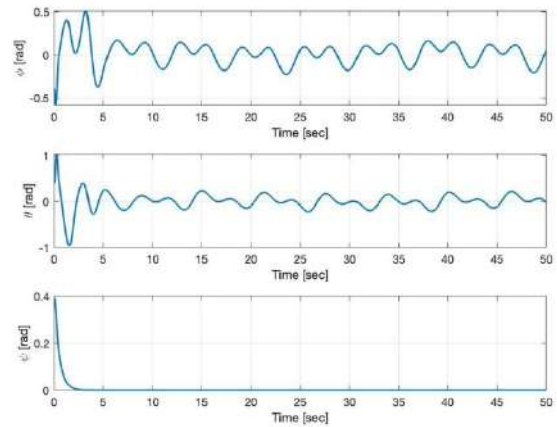


**Fig -2**: Three-dimensional trajectory of QR.
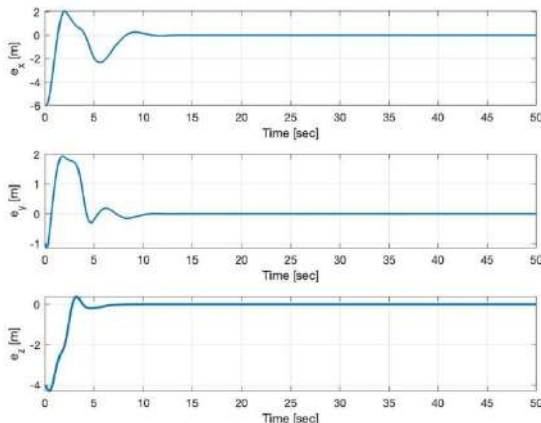


**Fig -3**: The tracking error of the position of QR



**Fig -4**: The control inputs.
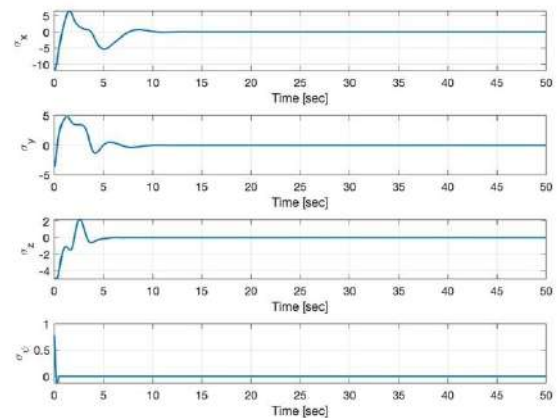


**Fig -5**: The Euler angles.



**Fig -6**: The sliding mode variables

### 5. CONCLUSIONS

This paper presents a novel single-loop control structure approach for controlling the quadrotor UAV. The single loop approach allows reducing the number of sensors while avoiding the time scale requirement imposed on multiple loop control systems. The efficacy of the proposed single-loop approach was demonstrated via simulations. The controllers have been designed in super twisting and continuous higher-

order sliding mode control form that has allowed achieving a high accuracy position tracking of the QR in the presence of the bounded perturbations. The tracking position and yaw errors were driven to zero asymptotically as seen in **Fig -3** and **Fig -5**. The single loop controller kept the angles roll and pitch in the secured range $\phi, \theta \in \left(-\frac{\pi}{2}, \frac{\pi}{2}\right)$. as seen in **Fig -5**.Future work will be focused on designing the adaptive continuous higher-order sliding mode controllers for quadrotor UAVs.

## References

[1] L. Salih, M. Moghavvemi, H. A. Mohamed, and K. S. Gaeid, "Modelling and PID controller design for a quadrotor unmanned air vehicle," in *2010 IEEE International Conference on Automation, Quality and Testing, Robotics (AQTR)*, 2010.

[2] H. Voos, "Nonlinear control of a quadrotor micro-UAV using feedback-linearization," in *2009 IEEE International Conference on Mechatronics*, 2009.

[3] Liu, J. Pan, Jian and Y. Chang, "PID and LQR trajectory tracking control for an unmanned quadrotor helicopter: Experimental studies," in *2016 35th Chinese Control Conference (CCC)*, 2016.

[4] Zhao, and B. Xian, Y. Zhang, and X. Zhang, "Nonlinear robust adaptive tracking control of a quadrotor UAV via immersion and invariance methodology," *IEEE Transactions on Industrial Electronics,* vol. 62, no. 5, pp. 2891--2902, 2014.

[5] T. Dierks, and S. Jagannathan, "Output feedback control of a quadrotor UAV using neural networks," *IEEE transactions on neural networks,* vol. 21, no. 1, pp. 50--66, 2009.

[6] L. Besnard , Y. B. Shtessel, and B. Landrum, "Quadrotor vehicle control via sliding mode controller driven by sliding mode disturbance observer," *Journal of the Franklin Institute,* vol. 349, no. 2, pp. 658-684, 2012.

[7] S. Esteban, F. Gordillo, and J. Aracil, "Three-time scale singular perturbation control and stability analysis for an autonomous helicopter on a platform," *International Journal of Robust and Nonlinear Control,* vol. 23, no. 12, pp. 1360--1392, 2013.

[8] L. Wang, and J. Su, "Trajectory tracking of vertical take-off and landing unmanned aerial vehicles based on disturbance rejection control," *IEEE/CAA Journal of Automatica sinica,* vol. 2, no. 1, pp. 65--73, 2015.

[9] W. Zhan, T. Tarn, and A. Isidori, "A canonical dynamic extension for noninteraction with stability for affine nonlinear square systems," *Systems \& control letters,* vol. 17, no. 3, pp. 177--184, 1991.

[10] K. Robenack, and S. Palis, "Nonlinear control of flat systems using a non-flat output with dynamic extension," in *2018 22nd International Conference on System Theory, Control and Computing (ICSTCC)*, 2018.

[11] A. Mokhtari, and A. Benallegue, "Dynamic feedback controller of Euler angles and wind parameters estimation for a quadrotor unmanned aerial vehicle," in *IEEE International Conference on Robotics and Automation, 2004. Proceedings. ICRA'04. 2004*, 2004.

[12] M. O. Efe, "Neural Network Assisted Computationally Simple PID Control of a Quadrotor UAV," *IEEE Transactions on Industrial Informatics,* vol. 7, no. 2, pp. 354--361, 2011.

[13] Y. Shtessel, C. Edwards, L. Fidman, and A. Levant, Sliding mode control and observation, Springer, 2014.

[14] Edwards, and Y. B. Shtessel, "Adaptive continuous higher order sliding mode control," *Automatica,* vol. 65, pp. 183-190, 2016.

[15] Bishop, R. C. Dorf and R. H., Modern Control Systems, vol. 13th ed, Boston: Pearson Education, 2016.